MODES OF A NONLINEAR FIBER CONTAINING A PARABOLIC GRADED-INDEX CORE WITH LIGHT INDUCED VARIABLE RADIUS

S.E. SAVOTCHENKO

Belgorod State Technological University named after V.G. Shukhov,
Kostukova St., 46, 308012 Belgorod, Russia
E-mail: savotchenkose@mail.ru

Received September 5, 2023

Abstract. New features of the light localization in a nonlinear and graded-index medium in the case of radial symmetry are described analytically. The model of nonlinear graded-index fiber assumes that the dielectric permittivity changes abruptly when the electric field amplitude reaches a certain level. The dielectric permittivity depends on the polar radius according to a parabolic law, in the regions where the electric field amplitude exceeds a certain level. Explicit exact solution to the wave equation is found, in terms of the Whittaker function and the modified Bessel function of the second kind, describing a new type of optical localized structure. The influence of the propagation constant and parameters of the nonlinear graded-index dielectric permittivity on the field profile over the fiber radius is analyzed. It is derived that the core radius and the dielectric permittivity of the core depend on the propagation constant. The dependence of the core radius on the propagation constant causes the appearance of local dispersion.

Key words: waveguide modes; waveguide optics; graded-index fiber; optical fiber; nonlinear fiber.

DOI: https://doi.org/10.59277/RomJPhys.2023.68.208

1. INTRODUCTION

Nonlinear fibers are widely used in many technical applications of optical telecommunication devices [1, 2]. Optical nonlinear effects in such fibers have recently been combined with the use of a gradient refractive index profile [3]. In particular, the Kerr nonlinearity is most often used [4]. The Kerr beam self-cleaning in lossless multimode fibers has been widely discussed [5, 6]. Nonlinear pulse propagation over a distance much larger than the dispersion distance satisfying the generalized nonlinear Schrödinger equation has been studied [7]. Many types of optical solitons in graded-index multimode fibers have been found [8, 9].

The authors of [10] noted the importance of the theoretical study of wave processes in nonlinear graded-index fibers. Various types of exact solutions to the wave equations were found in the case of circular cylindrical fibers [11, 12, 13]. The studies of the guided wave modes in such fibers are important for circular waveguides [14, 15]. It is necessary to study the features of light localization in circular fibers [16, 17] including wave localized structures in optical nonlinear media [18, 19]. Moreover, light wave propagation and light localization in photonic crystal fibers are actively studied for many years [20, 21, 22].

In the present paper, we study theoretically the modes of a nonlinear graded-index fiber. We find a new type of localized optical structure corresponding to the radial symmetric fundamental guided wave mode. To obtain an exact analytical solution to the wave equation in cylindrical coordinates we use a sharp-step model of nonlinear response [23, 24, 25]. The stepwise nonlinearity assumes that the dielectric constant or refractive index changes its value abruptly when the light intensity reaches a certain threshold value [26, 27, 28]. We have used recently this model to obtain exact analytical solutions to the wave equation in Cartesian coordinates for planar waveguides [29, 30, 31]. We also note that theoretical studies of combined gradient and nonlinear waveguide structures have become more active in recent years [32, 33, 34]; see also recent works on new types of nonlinear surface electromagnetic waves in diverse physical settings [35, 36, 37].

In this work, for the first time to the best of our knowledge, we theoretically describe the effect of combination the graded-index and nonlinear intensity-dependent properties of a cylindrical fiber. The main feature of the system under consideration is that the radius of the fiber, within which the medium is characterized by a parabolic profile of the dielectric permittivity, is not constant, but can vary depending on the optical parameters of the system and the propagation constant. We show that the dependence of the radius on the propagation constant causes the appearance of local dispersion.

This paper is organized as follows. The model of a nonlinear graded-index fiber with a light-induced core is formulated in Section 2. We find and analyze the exact solution of our model in Section 3. We discuss the dependence of the light induced core radius on the optical and propagation characteristics and the local dispersion estimation in Section 4. The conclusions are presented in Section 5.

2. MODEL OF A NONLINEAR GRADED-INDEX FIBER WITH A LIGHT-INDUCED CORE

We consider a nonmagnetic lossless fiber characterized by a nonlinear optical response and a graded-index region. The fiber axis coincides with the *z*-axis (longitudinal light propagation direction).

We consider the propagation of the transverse electric (TE) wave along the interface in the *z*-direction:

$$E = u\exp(i\beta z),$$

where β is the propagation constant, $k_0 = \omega/c$ is the wave number, ω is the wave frequency, c is the speed of light, and the function u in a weakly guiding circular fiber obeys the equation [38, 39]

$$\Delta_{\perp}u + (\varepsilon(r,u)k_0^2 - \beta^2)u = 0, \tag{1}$$

where

$$\Delta_{\perp} = \frac{1}{r}\frac{\partial}{\partial r}\left(r\frac{\partial}{\partial r}\right) + \frac{1}{r^2}\frac{\partial^2}{\partial \varphi^2}$$

is the Laplace operator in polar coordinates r and φ, $\varepsilon(r, u)$ is the dielectric permittivity of the nonlinear optical fiber [40, 41].

To find the exact analytical solution of Eq. (1) we use the simplest model of optical nonlinearity such a stepwise one [24]. The stepwise nonlinear response assumes that the fiber is characterized by the dielectric constant of ε_{cl} at low levels of the field intensity, and the dielectric constant abruptly changes its value to ε_{cor} when the electric field amplitude is larger than u_c. The core of a finite radius r_c is formed due the light wave propagation with the amplitude u_c. It is determined by the following condition $u(r_c) = u_c$.

Moreover, we suppose that the dielectric constant of the core depends on the distance from the fiber axis, *i.e.* on the polar radius r: $\varepsilon_{cor} = \varepsilon_{cor}(r)$, that is, we consider a graded-index fiber. We assume for definiteness that the dielectric constant of the core depends on the polar radius according to the parabolic law as

$$\varepsilon_{cor}(r) = \varepsilon_{co} - \Delta\varepsilon\left(\frac{r}{r_c}\right)^2, \qquad (2)$$

where ε_{cor} is the dielectric constant in the core axis, $\Delta\varepsilon$ is a change of the dielectric constant over the core.

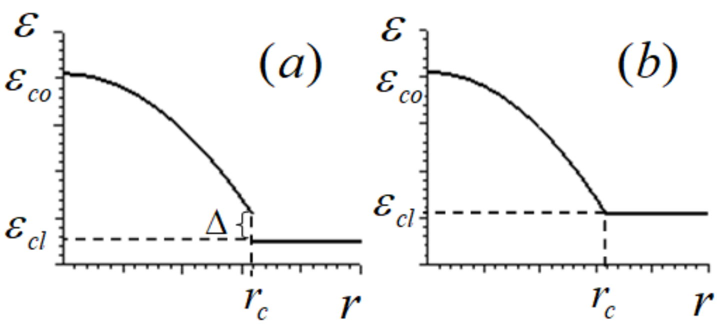

Fig. 1 – Schematic plot of the dielectric permittivity profiles defined by Eq. (3): (*a*) is the case of $\Delta_c = \varepsilon_{c0} - \varepsilon_{cl} \neq \Delta\varepsilon$, where $\Delta = |\Delta_c - \Delta\varepsilon|$; and (*b*) is the case of $\Delta\varepsilon = \Delta_c$.

Therefore, the dielectric permittivity can be written as a stepwise function describing the light-induced graded-index core in a weakly guiding circular fiber using a step-wise nonlinearity as

$$\varepsilon(r,u)=\begin{cases}\varepsilon_{cl}, u<u_c\\ \varepsilon_{cor}(r), u>u_c\end{cases} \tag{3}$$

where $\varepsilon_{cor}(r)$ is determined by Eq. (2).

The dielectric permittivity (3) combines the nonlinear and graded-index properties of the optical fiber. Note that in the general case the values of the dielectric constant at the field level u_c may be different (see Fig. 1*a*):

$$\Delta_c=\varepsilon_{c0}-\varepsilon_{cl}\neq\Delta\varepsilon.$$

In the case of continuous dependence of the dielectric permittivity (3) on the polar radius we have (see Fig. 1*b*):

$$\Delta\varepsilon=\Delta_c=\varepsilon_{co}-\varepsilon_{cl}.$$

Note that the refractive index is characterized by a sharp change in dependence on the intensity of the light flux in semiconductor crystals such as CdS and CdSe with the vanishingly small binding energy of biexcitons [42]. Combining such materials with spatially variable fluorine doping or varying the concentration of germania silica, for which a parabolic dependence of the refractive index is manufactured usually [43], one can obtain a stepwise nonlinear dependence similar to Eq. (3).

We consider only the field distribution having a radial symmetry, which corresponds to the fundamental mode. Therefore, considering $u=u(r)$ and combining Eqs. (1)–(3), we derive the wave equation inside the core where $u>u_c$:

$$\frac{\partial^2 u}{\partial r^2}+\frac{1}{r}\frac{\partial u}{\partial r}+\left(q^2-k_0^2\Delta\varepsilon\left(\frac{r}{r_c}\right)^2\right)u=0 \tag{4}$$

and the wave equation in the cladding where $u<u_c$:

$$\frac{\partial^2 u}{\partial r^2}+\frac{1}{r}\frac{\partial u}{\partial r}-\kappa^2 u=0, \tag{5}$$

where

$$q^2=\varepsilon_{co}k_0^2-\beta^2, \tag{6}$$

$$\kappa^2=\beta^2-\varepsilon_{cl}k_0^2. \tag{7}$$

We assume that the electric field is attenuated totally in the cladding before reaching the outer radius of the fiber, which can be realized when the core radius r_c

is much smaller than the fiber radius R ($r_c << R$). The radial distribution of the field obeys the conditions of limitation inside the fiber, vanishing at infinity: $u(r) \to 0$ at $r \to \infty$, and continuity of the field $u(r)$ and its derivative $u'(r)$ at the field level $u = u_c$. Therefore, the following boundary conditions can be used:

$$u(r_c - 0) = u(r_c + 0) = u_c, \tag{8}$$

$$u'(r_c - 0) = u'(r_c + 0). \tag{9}$$

Thus, the light localization in a graded-index fiber with a light-induced core is described by limited and continuous solution to Eqs. (4) and (5) satisfying the boundary conditions (8) and (9). We emphasize that the light induced core radius r_c formed at the field level u_c is an unknown function and will be determined by the optical parameters during the problem solving.

3. LIGHT LOCALIZED DISTRIBUTION

We find the limited at the origin solution to Eq. (4) in the case of $\beta^2 < \varepsilon_{co}k_0^2$:

$$u(r) = U_{co}\frac{M_{\mu,0}(r^2/r_G^2)}{r}, \tag{10}$$

where U_{co} is an unknown constant, $M_{\mu,0}(x)$ is the Whittaker function,

$$\mu = (qr_G/2)^2, \tag{11}$$

$$r_G^2 = r_c/k_0\sqrt{\Delta\varepsilon}. \tag{12}$$

The limited at infinity solution to Eq. (5) in the case of $\beta^2 > \varepsilon_{cl}k_0^2$ can be written as

$$u(r) = U_{cl}K_0(\kappa r), \tag{13}$$

where U_{cl} is an unknown constant and $K_0(x)$ is the modified Bessel function of the second kind.

After substituting solutions (10) and (13) into the boundary condition (8) we find the constants:

$$U_{co} = \frac{u_c r_c}{M_{\mu,0}(r_c^2/r_G^2)}, \tag{14}$$

$$U_{cl} = \frac{u_c}{K_0(\kappa r_c)}. \tag{15}$$

After substituting solutions (10) and (13) with the found constants (14) and (15) into the boundary condition (9) we obtain the equation

$$2\delta \frac{M'_{\mu,0}(\delta)}{M_{\mu,0}(\delta)} + \xi \frac{K_1(\xi)}{K_0(\xi)} = 1, \tag{16}$$

where

$$\xi = \kappa r_c,$$

$$\delta = r_c^2 / r_G^2 = r_c k_0 \sqrt{\Delta\varepsilon}\ .$$

Thus, we can write using Eqs. (10), (13)-(15) the exact solution to Eqs. (4) and (5) satisfying the boundary conditions (8) and (9) in the case of $\varepsilon_{cl} < (\beta/k_0)^2 < \varepsilon_{co}$ as follows

$$u(r) = u_c \begin{cases} \dfrac{r_c M_{\mu,0}(r^2/r_G^2)}{r M_{\mu,0}(r_c^2/r_G^2)}, u < u_c, \\ \dfrac{K_0(\kappa r)}{K_0(\kappa r_c)}, u > u_c. \end{cases}. \tag{17}$$

The solution (17) describes the electric field distribution symmetrically localized over the fiber diameter with core radius depending on the propagation constant and optical parameters of the fiber, which is determined by Eq. (16).

We derive from Eq. (17) that the field distribution at small radius (when $qr << 1$) decreases according to a parabolic law as

$$u(r) = u_0 \left(1 - \left(\frac{qr}{2}\right)^2\right), \tag{18}$$

where the field amplitude at the beam axis is given by

$$u_0 = u_c \delta / W_{\mu,0}(\delta). \tag{19}$$

We derive from Eq. (17) that the field distribution at a small distance from the fiber core (when $\kappa(r - r_c) << 1$) decreases according to a linear law as

$$u(r)=u_c\left(1-\frac{K_1(\xi)}{K_0(\xi)}\kappa(r-r_c)\right). \qquad (20)$$

Figure 2 demonstrates the influence of the optical parameters on the radial field distribution profile determined by Eq. (17). Figures 2*a* and 2*b* correspond to the case of continuous dielectric permittivity when $\Delta\varepsilon=\Delta_c$ (Fig. 1*b*) and Fig. 2*c* corresponds to the case of discontinuous dielectric permittivity when $\Delta\varepsilon\neq\Delta_c$ (Fig. 1*a*), and it suffers a jump of $\Delta=|\Delta_c-\Delta\varepsilon|$ at the field level u_c. The field increases with an increase in the propagation constant (Fig. 2*a*) and it decreases with an increase in the value of $\Delta\varepsilon$ (Fig. 2*b*) and with an increase in the value of Δ_c (Fig. 2*c*). The amplitude at the fiber axis defined by Eq. (19) increases with an increase in the propagation constant (Fig. 3*a*) and it decreases with an increase in the value of $\Delta\varepsilon$ (Fig. 3*b*).

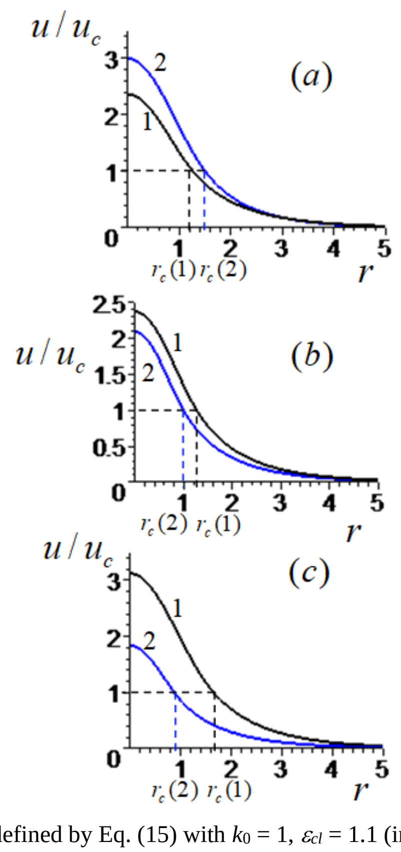

Fig. 2 – Field distribution defined by Eq. (15) with $k_0 = 1$, $\varepsilon_{cl} = 1.1$ (in dimensionless conventional units), (*a*) – $\Delta_c = \Delta\varepsilon$, $\varepsilon_{co} = \varepsilon_{cl} + \Delta\varepsilon$, $\Delta\varepsilon = 3$, $\beta = 1.3$ (1), $\beta = 1.4$ (2); (*b*) – $\Delta_c = \Delta\varepsilon$, $\varepsilon_{co} = \varepsilon_{cl} + \Delta\varepsilon$, $\beta = 1.3$, $\Delta\varepsilon = 3$ (1), $\Delta\varepsilon = 4$ (2); (*c*) – $\Delta_c \neq \Delta\varepsilon$, $\varepsilon_{co} = \varepsilon_{cl} + \Delta_c$, $\Delta\varepsilon = 3$, $\beta = 1.3$, $\Delta_c = 2.5$ (1), $\Delta_c = 4$ (2).

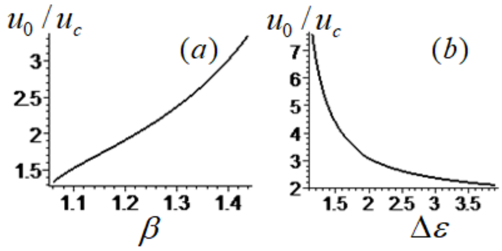

Fig. 3 – Dependencies of the amplitude at the fiber axis defined by Eq. (19) with $k_0 = 1$, $\varepsilon_{cl} = 1.1$: (*a*) – on the propagation constant β when $\Delta_c = \Delta\varepsilon$, $\varepsilon_{co} = \varepsilon_{cl} + \Delta\varepsilon$ with $\Delta\varepsilon = 3$; (*b*) – on the value of $\Delta\varepsilon$ when $\Delta_c = \Delta\varepsilon$, $\varepsilon_{co} = \varepsilon_{cl} + \Delta\varepsilon$ with $\beta = 1.3$.

4. DISCUSSION

The dependence of the core radius r_c on the optical and propagation characteristics is determined by Eq. (16). The analysis of Eq. (16) shows that the core radius increases with an increase in the propagation constant (Fig. 4*a*), and it decreases with an increase in the value of $\Delta\varepsilon$ in the case of continuous dielectric permittivity (Fig. 4*b*).

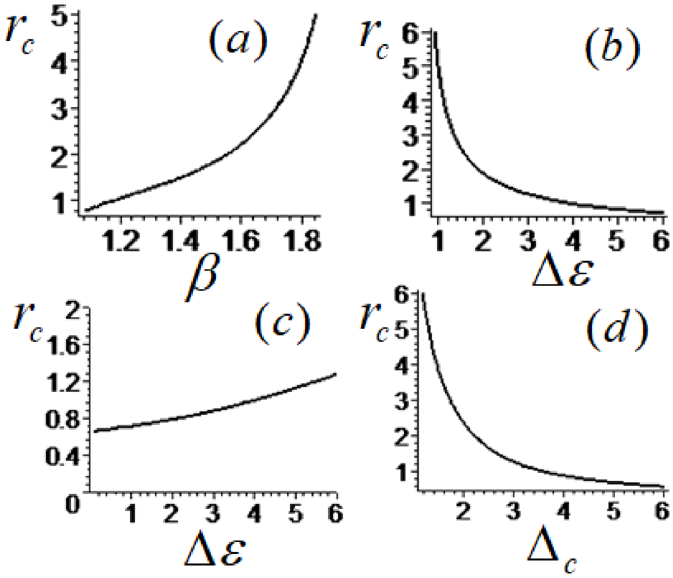

Fig. 4 – Dependencies of the core radius r_c determined by Eq. (16) with $k_0 = 1$, $\varepsilon_{cl} = 1.1$: (*a*) – on the propagation constant β when $\Delta_c = \Delta\varepsilon$, $\varepsilon_{co} = \varepsilon_{cl} + \Delta\varepsilon$ with $\Delta\varepsilon = 3$; (*b*) – on the value of $\Delta\varepsilon$ when $\Delta_c = \Delta\varepsilon$, $\varepsilon_{co} = \varepsilon_{cl} + \Delta\varepsilon$ with $\beta = 1.3$; (*c*) – on the value of $\Delta\varepsilon$ when $\Delta_c \neq \Delta\varepsilon$, $\varepsilon_{co} = \varepsilon_{cl} + \Delta_c$ with $\beta = 1.3$, $\Delta_c = 4$; (*d*) – on the value of Δ_c when $\Delta_c \neq \Delta\varepsilon$, $\varepsilon_{co} = \varepsilon_{cl} + \Delta_c$ with $\beta = 1.3$, $\Delta\varepsilon = 3$.

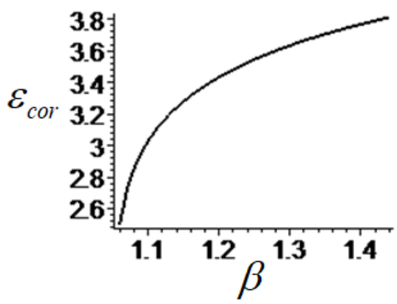

Fig. 5 – Dependence of the dielectric permittivity defined by Eq. (2) with substitution of the core radius calculated from Eq. (16) on the propagation constant β when $\Delta_c = \Delta\varepsilon$, $\varepsilon_{co} = \varepsilon_{cl} + \Delta\varepsilon$ with $k_0 = 1$, $\varepsilon_{cl} = 1.1$, $\Delta\varepsilon = 3$.

However, we observe the opposite trend of dependence on the value of $\Delta\varepsilon$ in the case of the discontinuous dielectric permittivity when r_c increases with an increase in the value of $\Delta\varepsilon$, when $\Delta\varepsilon$ and Δ_c are independent variable parameters (Fig. 4*c*). The core radius decreases as the change in the dielectric permittivity Δ_c increases (Fig. 4*d*).

It is important to note that the nonlinearity leads to local dispersion because the core radius depends on the propagation constant: $r_c = r_c(\beta)$. Therefore, the dielectric permittivity of the induced core depends on the propagation constant accordingly with Eq. (2): $\varepsilon_{cor} = \varepsilon_{cor}(r, \beta)$. Substituting the dependence of $r_c = r_c(\beta)$, calculated as a solution of Eq. (16) in Eq. (2), we obtain that the core dielectric permittivity increases with an increase in the propagation constant at any distances r inside the core (Fig. 5). It means that the derivative $\partial\varepsilon_{cor}/\partial\beta$ is positive when $u > u_c$.

If n is the refractive index and λ is the wavelength then we can define the local dispersion as

$$D = \frac{dn}{d\lambda}. \tag{21}$$

Using $\lambda = 2\pi/k$, Eq. (21) can be rewritten as

$$D = -\frac{k^2}{2\pi}\frac{dn}{dk}. \tag{22}$$

Then using $k = \beta n(\beta)$ we have

$$dk = d(\beta n(\beta)) = n d\beta + \beta dn = \left(n\frac{d\beta}{dn} + \beta\right)dn,$$

and Eq. (22) transforms into

$$D = -\frac{k^2}{2\pi}\frac{1}{n\dfrac{d\beta}{dn}+\beta} = -\frac{k^2}{2\pi}\frac{\dfrac{dn}{d\beta}}{n+\beta\dfrac{dn}{d\beta}}\,. \tag{23}$$

In a weak-guidance approximation

$$\beta\frac{dn}{d\beta} << n\,,$$

therefore, Eq. (23) transforms into

$$D = -\frac{k^2}{2\pi n}\frac{dn}{d\beta} = -\frac{n\beta^2}{2\pi}\frac{dn}{d\beta}\,. \tag{24}$$

Using $\varepsilon = n^2$, Eq. (24) can be written as

$$D = -\frac{\beta^2}{4\pi}\frac{d\varepsilon}{d\beta}\,. \tag{25}$$

Using Eq. (2) we obtain in the core

$$\frac{d\varepsilon}{d\beta} = \frac{2\Delta\varepsilon r^2}{r_c^3}\frac{dr_c}{d\beta}\,, \tag{26}$$

and the local dispersion (25) can be written as

$$D = -\frac{2\Delta\varepsilon(\beta r)^2}{2\pi r_c^3}\frac{dr_c}{d\beta}\,. \tag{27}$$

If we rewrite Eq. (16) as

$$F(\beta, r_c) = 0, \tag{28}$$

where

$$F(\beta, r_c) = 2\delta\frac{M'_{\mu,0}(\delta)}{M_{\mu,0}(\delta)} + \xi\frac{K_1(\xi)}{K_0(\xi)} - 1\,,$$

then we can find

$$\frac{dr_c}{d\beta} = -\left(\frac{\partial F}{\partial \beta}\right) / \left(\frac{\partial F}{\partial r_c}\right), \tag{29}$$

which can be substituted into Eq. (27).

Similarly, one can get the group velocity

$$V_{gr} = V_{ph}\left(\varepsilon + \frac{\beta}{2}\frac{d\varepsilon}{d\beta}\right), \tag{30}$$

where $V_{ph} = c/n$ is the phase velocity, c is the speed of light.

Thus, if the implicit dependence of the induced core radius on the propagation constant (Eq. (28)) is known, then it is possible to calculate the derivative (29), through which the local characteristics of dispersion and group velocity can be expressed.

5. CONCLUSIONS

We described analytically new features of the light localization in a nonlinear and graded-index medium in the case of radial symmetry. We proposed the model of nonlinear graded-index fiber, in which the dielectric permittivity changes abruptly when the electric field amplitude reaches a certain level. Moreover, we supposed that the dielectric permittivity depends on the polar radius according to a parabolic law in the regions where the electric field amplitude exceeds a certain level.

We obtained explicit exact solution to the wave equation in the terms of the Whittaker function and the modified Bessel function of the second kind, which describes the radial symmetric distribution of the strong transverse component of the electric field in a weak-guidance approximation. We analyzed the influence of the propagation constant and parameters of the nonlinear graded-index dielectric permittivity on the field profile over the fiber radius.

The core radius, in which the field amplitude exceeds a certain level, varies depending on the optical parameters of the system, in particular, on the propagation constant. As a result, the dielectric permittivity of the core depends on the propagation constant. We showed that the presence of such a dependence leads to the local dispersion that can be expressed in terms of the derivative of the core radius with respect to the propagation constant.

It is important to note that the waveguide structure proposed in our paper and the solutions obtained differ significantly from those reported in [44, 45]. The radius of the parabolic graded-index core can be varied and it is determined by the propagation constant and parameters of the parabolic law in contrast to the core radius considered in [44, 45], which is assumed to be a constant one.

We believe that results of this paper can be applied for manufacturing of the nonlinear graded-index optical fibers and complement the theory of the nonlinear and waveguide optics.

Acknowledgments. The study was carried out using equipment of the Center of High Technologies of the Belgorod V. G. Shukhov State Technological University.

REFERENCES

1. G. Agrawal, *Applications of Nonlinear Fiber Optics*, Academic Press, 2008.
2. I. P. Kaminow, T. Li, A. E. Willner (Editors), *Optical Fiber Telecommunications VIB*, in *Optics and Photonics, Optical Fiber Telecommunications*, Academic Press, 2013.
3. K. Krupa, A. Tonello, A. Barthélémy, T. Mansuryan, V. Couderc, G. Millot, P. Grelu, D. Modotto, S. A. Babin, S. Wabnitz, APL Photonics **4**(11), 110901 (2019).
4. G. Agrawal, *Nonlinear Fiber Optics*, 6th Edition, Academic Press, 2019.
5. R. Guenard, K. Krupa, R. Dupiol, M. Fabert, A. Bendahmane, V. Kermene, A. Desfarges-Berthelemot, J. L. Auguste, A. Tonello, A. Barthélémy, G. Millot, S. Wabnitz, V. Couderc, Opt. Express **25**, 4783–4792 (2017).
6. E. Deliancourt, M. Fabert, A. Tonello, K. Krupa, A. Desfarges-Berthelemot, V. Kermene, G. Millot, A. Barthélémy, S. Wabnitz, V. Couderc, OSA Continuum **2**, 1089–1096 (2019).
7. A. Mafi, J. Lightwave Technol. **30**, 2803–2811 (2012).
8. W. H. Renninger, F. W. Wise, Nat. Commun. **4**, 1719 (2013).
9. A. S. Ahsan, G. P. Agrawal, Opt. Lett. **43**, 3345–3348 (2018).
10. P. Horak, F. Poletti, *Multimode nonlinear fibre optics: Theory and applications*, in *Recent Progress in Optical Fiber Research*, edited by M. Yasin, S. W. Harun, H. Arof, IntechOpen, 2012.
11. N. Zhang, Y. Y. Lu, Opt. Lett. **46**, 4410–4413 (2021).
12. K. Morishita, IEEE Transactions on Microwave Theory and Techniques **31**(4), 344–350 (1983).
13. C. Yeh, IEEE Transactions on Education **E-30**(1), 43–51 (1987).
14. Y. Kato, M. Miyagi, IEEE Transactions on Microwave Theory and Techniques **40**(4), 679–685 (1992).
15. H. Shu, M. Bass, Journal of Lightwave Technology **25**(9), 2693–2699 (2007).
16. M. Ghulinyan, L. Pavasi, *Light Localization and Lasing*, Cambridge University Press, Cambridge, United Kingdom, 2015.
17. D. Nolan, D. T. Nguyen, Front. Phys. **9**, 713085 (2021).
18. B. A. Malomed, D. Mihalache, Rom. J. Phys. **64**, 106 (2019).
19. D. Mihalache, Rom. Rep. Phys. **73**, 403 (2021).
20. J. C. Knight, T. A. Birks, R. F. Cregan, P. St. J. Russell, J.-P. de Sandro, Opt. Mater. **11**, 143–151 (1999).
21. *Basics of photonic crystal fibers*, in: *Photonic Crystal Fibers. Materials Science*, Vol. 102, Springer, Dordrecht, 2007.
22. D. Novoa, N. Y. Joly, Crystals **11**, 739 (2021).
23. A. E. Kaplan, Phys. Rev. Lett. **55**, 1291–1294 (1985).
24. E. Kaplan, IEEE J. of Quantum Electronics **QE-21** 1538–1543 (1985).
25. R. H. Enns, S. S. Rangnekar, A. E. Kaplan, Phys. Rev. A **36**, 1270 (1987).
26. P. I. Khadzhi, L. V. Fedorov, Phys. Tech. Lett. **61**, 110–113 (1991).

27. N. N. Beletsky, E. A. Hasan, Phys. of the Sol. St. **36**, 647–652 (1994).
28. K. D. Lyakhomskaya, P. I. Hadji, Tech. Phys. **70**, 86–90 (2000).
29. S. E. Savotchenko, Journal of Optics **22**, 065504 (2020).
30. S. E. Savotchenko, Rom. J. Phys. **65**, 202 (2020).
31. S. E. Savotchenko, Tech. Phys. Lett. **46**, 823–826 (2020).
32. A. J. Hussein, Z. M. Nassar, S. A. Taya, Microsyst. Technol. **27**, 2589–2594 (2021).
33. S. A. Taya, A. J. Hussein, O. M. Ramahi, I. Colak, Y. B. Chaouche, J. Opt. Soc. Am. B **38**, 3237–3243 (2021).
34. A. H. M. Almawgani, A. J. Hussein, S. A. Taya, A. T. Hindi, I. Colak, Anas A. M. Alqanoo, S. Patel, A. Pal, J. Phys. A: Math. Theor. **56**, 235203 (2023).
35. S. E. Savotchenko, Rom. J. Phys. **67**, 202 (2022).
36. S. E. Savotchenko, Rom. J. Phys. **66**, 201 (2021).
37. S. E. Savotchenko, Rom. Rep. Phys. **74**, 407 (2022).
38. D. Gloge, Appl. Opt. **10**, 2252–2258 (1971).
39. S. Pillay, D. Kumar, H. Rashid, Journal of Electromagnetic Analysis and Applications **5**(8), 333–335 (2013).
40. M. J. Adams, *An Introduction to Optical Waveguides*, Wiley, Chichester, 1981.
41. C-L. Chen, *Foundations for guided-wave optics*, John Wiley & Sons, Inc., 2005.
42. O. V. Korovai, P. I. Khadzhi, Phys. Solid State **45**, 386–390 (2003).
43. M. Lancry, B. Poumellec, A. Chahid-Erraji, M. Beresna, P. G. Kazansky, Opt. Mater. Express **1**, 711–723 (2011).
44. T. K. Lim, B. K. Garside, J. P. Marton, Opt. Quant. Electron. **11**, 329–344 (1979).
45. R. L. Lachange, P.-A. Belanger, J. Lightwave Techn. **9**(11), 1425 (1991).